E3S Web of Conferences **111**, 01057 (2019) https://doi.org/10.1051/e3sconf/201911101057
CLIMA 2019

Numerical study of the effect of wind on the cooling of photovoltaic panels

Dakouo Koita[1,2,3], *Catalin-Viorel Popa*[1], *Bruno Robert*[3] *and Catalin-Daniel Galatanu*[4,*]

[1]GRESPI EA 4694, Université de Reims Champagne-Ardenne, Reims, France

[2]École Nationale d'Ingénieurs Abderhamane Baba TOURE, Mali

[3]CRESTIC EA 3804, Université de Reims Champagne-Ardenne, Reims, France

[4]Faculty of Civil Engineering and Building Equipment, Technical University of Iasi, Romania

Abstract. The main objective of this study is to optimize the production of electricity from a photovoltaic (PV) plant with a capacity of 50MWc. The power plant is located near the city of KITA, Mali, in an area whose climate is characterized by high temperatures. However, the temperature of photovoltaics cells plays a key role in their performance, which deteriorates when the temperature increases. In this study we focus on the analysis of laminar forced convection flow around a PV panel, main element of a photovoltaic plant, considering the ambient temperature, irradiation as well as the velocity and the direction of the wind. Several operating configurations were analysed in relation to the specific climatic conditions of Mali for a typical day of sunshine with a daily irradiation of a duration of 12 hours between 6:00 and 18:00. The mass transport, momentum and energy equations are solved numerically using the finite volume method. This method is based on the spatial integration of transport equations with respect to elementary control volumes. Computer simulations are performed with ANSYS Fluent® CFD commercial software. Our results show that considering the effect of wind plays an important role in the temperature estimates of photovoltaic cells and that accurate knowledge of this behaviour is essential for optimizing production.

1 Introduction

Solar energy is the cleanest and most sustainable source of energy available to a large majority of the world's population. The solar energy received by the Earth is abundant and inexhaustible. Approximately, the solar continuous power reaching the earth's surface is about 120000 TW [1]. Each year, it corresponds to a potential 6,500 times greater than the amount of energy yearly required in the world. Indeed, in 2014, world primary energy consumption stood at 13684 Mtoe that are equivalent to 159000 TWh [2]. Only a small part of this energy is exploited by man for his daily needs. The industrial production of solar electricity falls into two sectors: solar photovoltaic production and solar thermal generation. The photovoltaic sector contributes exclusively to the generation of electrical energy by means of photovoltaic solar panels while the thermal sector contributes not only to the generation of electric power by means of a superheated steam turbine but also to the production of water hot sanitary or heat production to warm the buildings. The electrical performance of the photovoltaic generators (PV) are strongly dependent on the operating temperature. It is known that the no-load voltage decreases with the temperature rise of the PV cell, and that, to a lesser extent, the photovoltaic current increases with it. This results in a significant decrease in the maximum power available when the temperature of the PV cell increases. The technical documentation of the photovoltaic panels indicates two coefficients making it possible to correct the principal characteristics in a proportional way. These characteristics are defined under standard test conditions (STC) including, among others, ambient temperature. This approach makes it possible to obtain results which are ordinarily satisfactory although not very precise. Indeed, the photoelectric phenomenon is very sensitive to the temperature of the semiconductor crystal in which it occurs. The cell is trapped between different layers of materials, achieving among other things, the optical treatment and giving it its mechanical strength. It is therefore proposed to precede the electrical simulation of the generator with a thermal study, in order to evaluate the temperature of the photovoltaic cells more precisely. Therefore, we focus in this study on the analysis of laminar forced convection flow around a PV panel, the main component of a photovoltaic power plant. Regardless of the accuracy improvement in the estimation of cell temperature, this approach will also allow us to consider the influence of wind on the performance of PV panels, which is not possible with the classic approach based on the ambient temperature.

* Corresponding author: catalin.galatanu@tuiasi.ro

 https://doi.org/10.1051/e3sconf/201911101057

During the operation of the PV modules, their cells heat up due to a number of phenomena such as thermalization, charge carrier recombination, the Joule effect, the Peltier effect and the Thomson effect. Knowledge of photovoltaic cell temperature is of significant importance in predicting the efficiency that the PV system can achieve during operation. Zondag et al. [3] found that a lower temperature of the PV module improves its efficiency. Moreover, the heating of the PV panels can be attenuated by the flow of air around the panel, wind-induced flow [4]. Edgar et al. [5] show that passive convection cooling of PV modules can improve electrical power by 2% under nominal operating conditions. Goverde et al [6] conducted an experimental study varying the irradiation of the PV panel and the wind speed between 1 and 5 m/s. They found that the temperature of the module as well as the coefficient of convective heat transfer were significantly affected by the wind. In addition, analytical models have been proposed to evaluate cell temperature as a function of wind velocity [7-8]. Stropnik and Stritih [9] focused on increasing electrical efficiency and power output of photovoltaic (PV) panel with the use of a phase change material (PCM). They found that the maximum temperature difference on the surface of PV panel without PCM was 35.6 °C higher than on a panel with PCM in a period of one day.

Our work is part of a program of scientific cooperation with Mali, with the objective of optimizing the electricity production of a 50 MWp photovoltaic power plant located in KITA in the area Sahel-Saharan Africa, where the climate is characterized by high temperatures. To achieve this objective, it is suitable to set the physical relationship between the temperature of the PV cell, the illumination and the relevant meteorological parameters such as wind is the most important factor influencing the cell temperature.

2 Problem setup

In this study, we focus on the analysis of laminar forced convection flow around a PV panel, main element of a photovoltaic plant, considering the ambient temperature, irradiation as well as the velocity and the direction of the wind. Several operating configurations were analysed in relation to the specific climatic conditions of Mali for a typical day of sunshine with a daily irradiation of a duration of 12 hours between 6:00 and 18:00.

2.1. Geometry

The photovoltaic panel (Fig. 1) used for the numerical simulations has the following dimensions: length L = 1.65 m, width l = 0.992 m and thickness H = 6.243 mm. The PV panel consists of 9 layers (Table 1) and is placed at the top of an aluminium frame 40 mm high, 35 mm width and 8 mm thick (Fig. 2).

In the case of the KITA photovoltaic plant, the climatic conditions in Mali require the installation of PV panels at 2 m from the ground with an inclination of 15° relative to the horizontal as well as with an orientation of 7° East compared to south in the horizontal plane (xy). The fluid domain around the PV panel (Fig. 3) is constructed to ensure the independence of the solution from the boundaries and extends 3 m upstream, left, right and top and 9 m downstream [10].

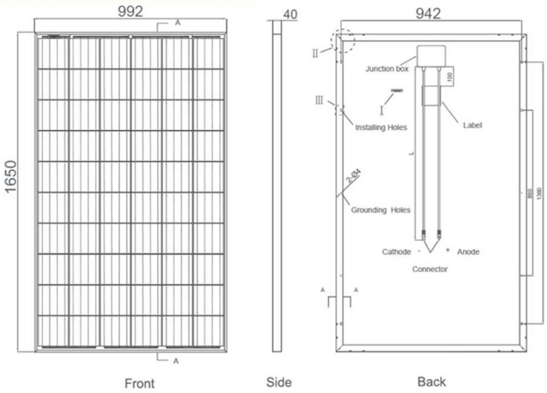

Fig. 1. Photovoltaic panel

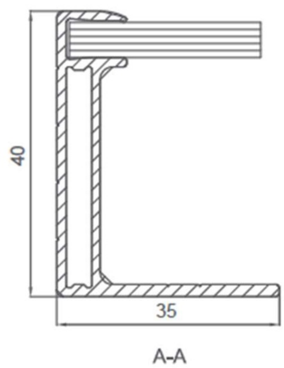

Fig. 2. Integration of the PV panel into the aluminium frame

Table 1. PV Panel Properties.

Layer	*Material*	*Thickness (mm)*	ρ $\left(\frac{kg}{m^3}\right)$	*Cp* $\left(\frac{J}{Kg.K}\right)$	*k* $\left(\frac{W}{m.K}\right)$
1	*Glass*	*3.2*	*2500*	*500*	*1.1*
2	*Encapsulant 3M*	*0.45*	*955*	*2090*	*0.311*
3	*Encapsulant first*	*0.5*	*860*	*2090*	*0.311*
4	*PV Cell*	*0.208*	*2330*	*677*	*130*
5	*Encapsulant 3M*	*0.45*	*911*	*2090*	*0.311*
6	*Encapsulant first*	*0.5*	*820*	*2090*	*0.311*
7	*Tedlar TPE*	*0.345*	*1400*	*1250*	*0.15*
8	*Tedlar TFB*	*0.3*	*1100*	*1250*	*0.15*
9	*Tedlar TPF*	*0.29*	*1400*	*1250*	*0.15*

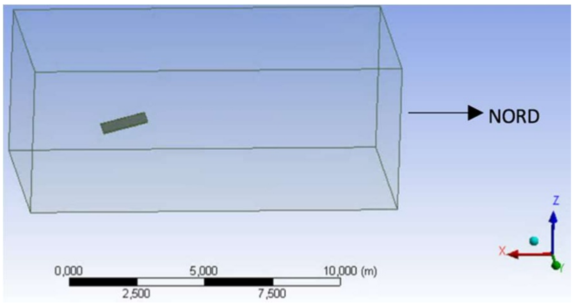

Fig. 3. Geometry of fluid domain

In order to validate the mesh, we tested 3 different meshes (Table 2).

Table 2 Mesh independence

Mesh	Coarse (n° 1)	Normal (n° 2)	Fine (n° 3)
Number of cells	12 million	39 million	47 million

Finally, we chose the mesh n° 2 which represents a good compromise between solution accuracy and the computation time. The structured mesh of the fluid domain (Fig. 4) comprising 39 million cells is, on the one hand, of boundary layer type near the PV panel and, on the other hand, progressive away from the PV panel.

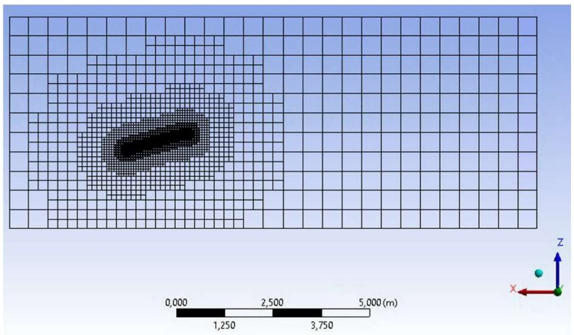

Fig. 4. Mesh of fluid domain

2.2 Physical model

The physical model of forced convection airflow around the photovoltaic panel includes the transport equations of mass, momentum and energy (Eq. 1 – 5). We consider the flow as laminar, steady and three-dimensional. The governing equations are:

- Continuity equation:

$$\frac{\partial \rho}{\partial t}+\frac{\partial \rho u}{\partial x}+\frac{\partial \rho v}{\partial y}+\frac{\partial \rho w}{\partial z}=0 \quad (1)$$

- Momentum equations:

$$\left(\frac{\partial u}{\partial t}+u\frac{\partial \rho u}{\partial x}+v\frac{\partial \rho u}{\partial y}+w\frac{\partial \rho u}{\partial z}\right)=-\frac{\partial P}{\partial x}+\frac{\partial}{\partial x}\left(\mu\frac{\partial u}{\partial x}\right)+\frac{\partial}{\partial y}\left(\mu\frac{\partial u}{\partial y}\right)+\frac{\partial}{\partial z}\left(\mu\frac{\partial u}{\partial z}\right)+\frac{\partial u}{\partial x}\frac{\partial \mu}{\partial x}+\frac{\partial v}{\partial x}\frac{\partial \mu}{\partial y}+\frac{\partial w}{\partial x}\frac{\partial \mu}{\partial z} \quad (2)$$

$$\left(\frac{\partial v}{\partial t}+u\frac{\partial \rho v}{\partial x}+v\frac{\partial \rho v}{\partial y}+w\frac{\partial \rho v}{\partial z}\right)=-\frac{\partial P}{\partial y}+\frac{\partial}{\partial x}\left(\mu\frac{\partial v}{\partial x}\right)+\frac{\partial}{\partial y}\left(\mu\frac{\partial v}{\partial y}\right)+\frac{\partial}{\partial z}\left(\mu\frac{\partial v}{\partial z}\right)+\frac{\partial u}{\partial y}\frac{\partial \mu}{\partial x}+\frac{\partial v}{\partial y}\frac{\partial \mu}{\partial y}+\frac{\partial w}{\partial y}\frac{\partial \mu}{\partial z} \quad (3)$$

$$\left(\frac{\partial w}{\partial t}+u\frac{\partial \rho w}{\partial x}+v\frac{\partial \rho w}{\partial y}+w\frac{\partial \rho w}{\partial z}\right)=-\frac{\partial P}{\partial z}-\rho g+\frac{\partial}{\partial x}\left(\mu\frac{\partial w}{\partial x}\right)+\frac{\partial}{\partial y}\left(\mu\frac{\partial w}{\partial y}\right)+\frac{\partial}{\partial z}\left(\mu\frac{\partial w}{\partial z}\right)+\frac{\partial u}{\partial z}\frac{\partial \mu}{\partial x}+\frac{\partial v}{\partial z}\frac{\partial \mu}{\partial y}+\frac{\partial w}{\partial z}\frac{\partial \mu}{\partial z} \quad (4)$$

- Energy equation:

$$\rho C_p\left(\frac{\partial T}{\partial t}+u\frac{\partial T}{\partial x}+v\frac{\partial T}{\partial y}+w\frac{\partial T}{\partial z}\right)=\frac{\partial}{\partial x}\left(k\frac{\partial T}{\partial x}\right)+\frac{\partial}{\partial y}\left(k\frac{\partial T}{\partial y}\right)+\frac{\partial}{\partial z}\left(k\frac{\partial T}{\partial z}\right) \quad (5)$$

The fluid is considered to be newtonian, and the physical properties (ρ, Cp, k, μ) of the fluid are temperature dependent. Indeed, the Boussinesq approximation is not valid for air with temperature variations higher than 10 K [11].

The radiation heat transfer is not considered in the physical model because the location of the PV panels in the solar track with no surrounding reflective surfaces, makes this mode of heat transfer insignificant. Moreover, on the overall irradiation received by the PV panel, only 31.9% of this energy is converted into heat and will contribute to the heating of the PV cell [12]. The soil temperature was taken 2K higher than the ambient temperature to consider its heating due to direct solar radiation [5].

Table 3 Climate conditions on April 01, 2013 in Kita, Mali.

Hour	**ϕ** $\left(\frac{W}{m^2}\right)$	T_{amb} **(K)**	**V** $\left(\frac{m}{s}\right)$	**Wind direction from south (°)**
6h30	174	291.85	1.4	291
7h30	434	299.85	2.5	280
8h30	685	303.75	2.7	289
9h30	897	308.25	2.5	300
10h30	1039	311.85	2.2	313
11h30	1102	314.55	2,1	328
12h30	1075	315.65	2	337
13h30	967	315.65	2.1	333
14h30	780	315.15	2.2	332
15h30	539	314.05	2.2	334
16h30	278	312.25	2.1	333
17h30	49	305.75	1.9	330
Average values	**668**	**309**	**2.2**	**317**

The boundary conditions corresponding to the several cases studied for a typical day (01 April 2013) consider the specific climatic conditions of Mali (Table 3). The choice of the typical date was made after analysis of the meteo data over 20 years between 1994 and 2014 for this geographical area. The daily irradiation of a duration of 12 hours is between 6:00 and 18:00.

2.3 Numerical method

Transport equations of mass, momentum and energy (1) – (5) are solved numerically using the finite volume method [13]. This method is based on the spatial integration of transport equations on control volumes. The coupling between velocity and pressure is achieved with the coupled algorithm that solves the equations of continuity and momentum simultaneously and gives an advantage to treat flows with a strong interdependence between dynamic and thermal fields. Central-Differenced Schemes and Second-Order Upwind Schemes are used for the spatial discretization for diffusive terms and convective terms respectively. The convergence criteria were based on the absolute residuals resulting from the integration of the conservation equations over finite control volumes. For all simulations performed in this study, converged solutions were achieved after a residuals decrease lower than 10^{-3} for all the governing equations. 3D numerical simulations are performed with ANSYS Fluent® CFD commercial software.

3 Results and discussion

The efficiency of the PV cell is generally measured under standard test conditions (STC) with a PV cell temperature of 25 °C and an irradiation of 1000 $\frac{W}{m^2}$. These conditions are rarely met in outdoor facilities. The numerical model developed in this study represents a tool for the analysis of the operating temperature of photovoltaic generators. In this study, we present the results for a typical day using the specific climatic conditions of Mali, the ambient temperature, the irradiation as well as the velocity and direction of the wind. The typical day of sunshine in Mali with a daily irradiation of a duration of 12 hours between 6:00 and 18:00. For example, the solar radiation at 6:30 and 17:30 on the city of Kita is respectively 174 $\frac{W}{m^2}$ and 49 $\frac{W}{m^2}$.

Figures 5, 6 and 7 show the PV module isotherms for 3 representative cases of a typical day, that is to say, 7:30, 11:30 and 15:30. The temperature of the PV cell, which can be assumed to be identical to the temperature of the PV module [14], shows great variability under changing outdoor conditions. During a cloudless summer day in Mali in the town of Kita, the cell temperature is between 309K and 341K over a day. The maximum temperature of 341K is reached at 11h30 when the daily irradiation is maximum and when the wind blows from the south-east direction (328°) with a velocity close to the average day velocity. This heating of the PV cells can lead to a considerably reduced energy efficiency. It is also observed that despite a substantially constant ambient temperature from 11:30 to 15:30, the temperature of the PV panel at 15:30 is only 324K. The cooling of the PV cell is due to the higher wind velocity and its more favorable orientation compared to prevailing winds.

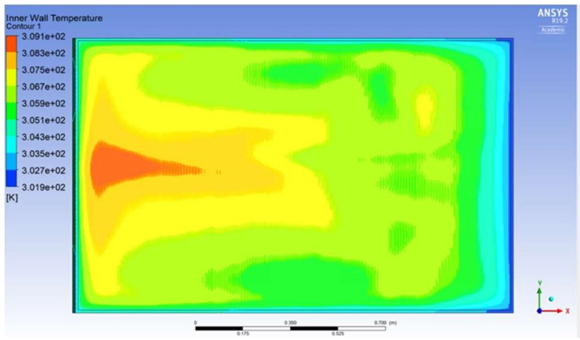

Fig. 5. Temperature of the PV panel at 7:30 (top view)

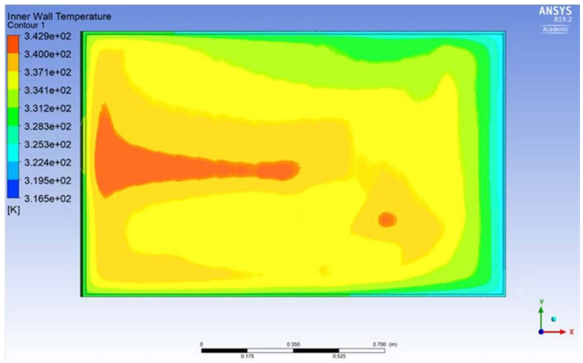

Fig. 6. Temperature of the PV panel at 11:30 (top view)

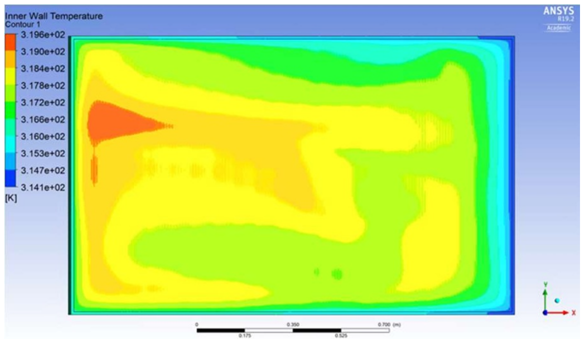

Fig. 7. Temperature of the PV panel at 16:30 (top view)

Figure 8 shows the streamlines in the median plane, parallel with the x axis, around the PV panel at 07:30, 11:30 and 16h30 respecting the specific climatic conditions (Table 3).

Knowing that the PV panel is installed in the upper part of the supporting aluminium frame (Fig. 2) and considering the inclination and the position of the PV panel in relation to the ground, a recirculation zone creates at the bottom of the underside of the PV panel, whatever time of day. Consequently, the airflow in this area is characterized by low velocities, which promote a significant heating of the cells located at the bottom of the underside of the PV panel.

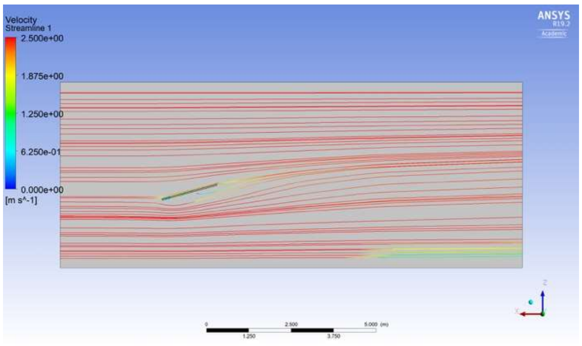

(a)

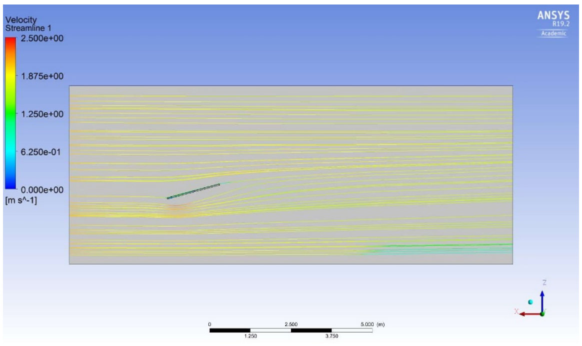

(b)

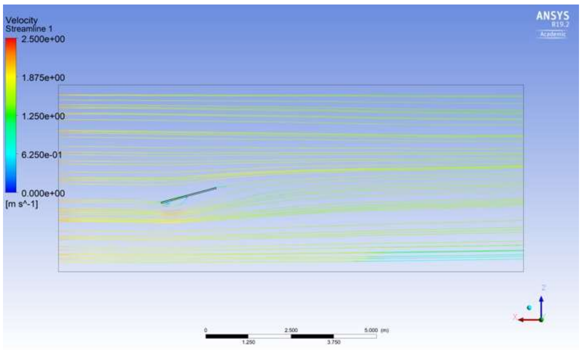

(c)

Fig. 8. Streamlines in the median plane, parallel with the x axis, at 07:30 (a), 11:30 (b) and 16:30 (c)

In a second part, two additional inclinations of the PV panel (10° and 20° relative to the horizontal) were tested in order to study the influence of the inclination of the PV panel with respect to its heating, knowing that initially the PV panel was tested for à 15° inclination. These inclinations relative to the horizontal were tested for the most adverse climatic conditions, i.e. at 11:30 during a typical day.

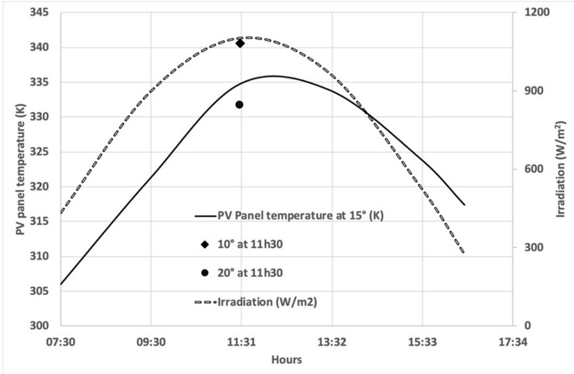

Fig. 9. Daily evolution of panel PV temperature at 15° and irradiation and the variation of the temperature at 11:30 for different inclinations (10° and 20°)

Figure 9 represents the evolution of the temperature during the typical day of April 01, 2013 for the corresponding irradiations and an inclination of 15° of PV panel. In addition, the influence of the inclination of the PV panel relative to the horizontal is displayed for 2 inclinations (10° and 20°). One may note that the temperature evolution follows local irradiation with a maximum reached at 11:30. Moreover, it is found that, for a greater inclination (20°) relative to the horizontal than that initially tested (15°), the PV panel subjected to the same climatic conditions is colder than 3K.

4 Conclusion

A 3D numerical study of laminar forced convection airflow around a photovoltaic panel was conducted. Several operating configurations were analysed compared to changing climatic conditions in Mali for a typical day. During a cloudless summer day in the city of Kita in Mali and for an inclination of the PV panel relative to the horizontal of 15°, the cell temperature changes from 309K and 341K. For these climatic conditions, the maximum temperature is reached at 11:30. Despite the fact that the ambient temperature remains high until 15:30, the temperature of the PV cell drops thanks to the airflow generated by the wind around PV panel. Moreover, it is found that, for a greater inclination (20°) relative to the horizontal than that initially tested (15°), the PV panel subjected to the same climatic conditions is colder than 3K. Our results show that considering the effects of wind and PV panel inclination plays an important role in the temperature estimates of photovoltaic cells. Work continues on electrical modelling to find a physical relationship between the temperature of the PV cell, the irradiation received and the wind velocity and direction.

Nomenclature

C_p	specific heat capacity, $\frac{J}{kg.K}$
g	acceleration of gravity, $\frac{m}{s^2}$
k	thermal conductivity, $\frac{W}{m.K}$
P	static pressure, Pa
T	temperature, K
t	time, s
u,v,w	velocity components, $\frac{m}{s}$
x,y,z	coordinates, m

Greek symbols

ϕ	heat flux density, $\frac{W}{m^2}$
ρ	density, $\frac{kg}{m^3}$
μ	dynamic viscosity, Pa.s

Acknowledgements

The authors express their gratitude to the French Ministry of Foreign Affairs and Akuo Energy Company for its technological expertise. C.D.G. thanks to the colleagues involved in grant PCAI-163CI, contract PN-III-P2-2.1-CI-2018-0965 for imaging measurement, grant SILUM-219CI, contract PN-III-P2-2.1-CI-2018-1287 for luminance measurement, grant MAXLUM-256CI, contract PN-III-P2-2.1-CI-2018-1490 for simultaneous imaging measurement of correlated colour temperature and luminance.

References

1. O. Morton *A new day dawning?: Silicon Valley sunrise,* Nature, **443**, 19–22 (2006)
2. *International Energy Agency (IEA).* World Energy Outlook, 6-61 (2016)
3. H.A. Zondag, D.W. De Vries, WGJ Van Helden, RJC Van Zolengen, AA. Van Steenhoven *The thermal and electrical yield of a PV-thermal collector*, Solar Energy **72** (2), 113-128 (2002)
4. N. Boulfaf, J. Chaoufi *Identification of Thermal Parameters of a Solar Photovoltaic Panel in Three-Dimensional using Finite Element Approach*, International Journal of Renewable Energy Research **7** (2), 578-584 (2017)
5. R. Edgar, S. Cochard, Z. Stachurski *A computational fluid dynamic study of PV cell temperatures in novel platform and standard arrangements*, Solar Energy **144**, 203 -214 (2017)
6. H. Goverde, D. Goossens, J. Govaerts, F. Catthoor, K. Baert, J. Poortmans, J. Driesen *Spatial and temporal analysis of wind effects on PV modules: Consequences for electrical power evaluation*, Solar Energy **147**, 292-299 (2017)
7. M. Koehl, M. Heck, S. Wiesmeier, J. Wirth *Modeling of the nominal operating cell temperature based on outdoor weathering*, Solar Energy Materials and Solar Cells **95** (7), 1638-1646 (2011)
8. M. Akhsassi, A. El Fathi, N. Erraissi, N. Aarich, A. Bennouna, A., M. Raoufi, A. Outzourhit *Experimental investigation and modeling of the thermal behavior of a solar PV module*, Solar Energy Materials and Solar Cells **180**, 271-279 (2018)
9. R. Stropnik, U. Stritih, *Increasing the efficiency of PV panel with the use of PCM*, Renewable Energy, **97**, 671-679 (2016)
10. Popa C.V., Zaidi H., Arfaoui A., Polidori G., Taiar R., Fohanno S. *Wall shear stress analysis around a competitive swimmer using 3D Navier-Stokes equations in CFD*, Acta of Bioengineering and Biomechanics, **13** (1), 3 – 11 (2011)
11. D.D. Gray, A. Giorgini *The validity of the Boussinesq approximation for liquids and gases*, International Journal of Heat and Mass Transfer **19**, 545-551 (1976)
12. O. Dupre, M. Amara, et R. Vaillon *TASC-1D-cSi: A simulation tool to scrutinize the thermal impacts on the performances of crystalline silicon solar cells*, eprint: arXiv, no 1306.5723, p. 11 (2013)
13. S.V. Patankar *Numerical heat transfer and fluid flow* (Hemisphere Publishing Corporation, Mc. Graw Hill Book Company, 1980)
14. M. Mattei, G. Notton, G. Cristofari, M. Muselli, P. Poggi *Calculation of the polycrystalline PV module temperature using a simple method of energy balance* Renewable Energies **31**, 553-567 (2006)